Oxide Dispersion Strengthening of Eurofer97 Steel for fusion

Tay Sparks[a], Michael Gorley[b], Thomas Connolley[c], Yiqiang Wang[b], Biao Cai[a]

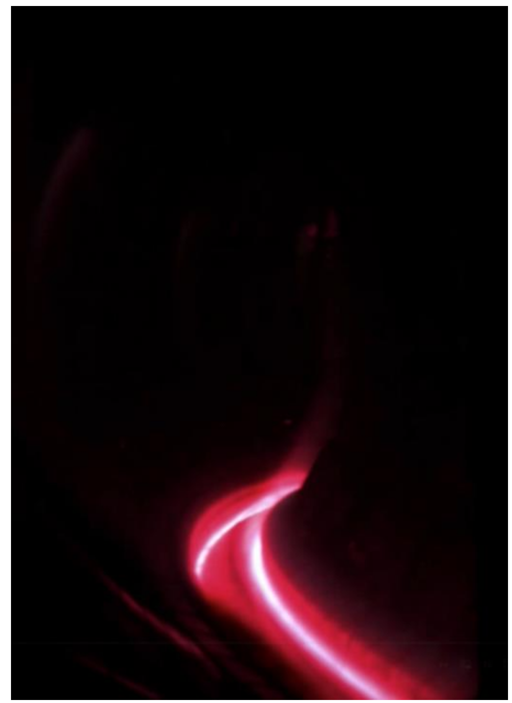

[a]School of Metallurgy and Materials, University of Birmingham
[b]UK Atomic Energy Authority, Culham Science Centre
[c]Diamond Light Source Ltd, Harwell Science and Innovation Campus

Dr Biao Cai, b.cai@bham.ac.uk
Dr Yiqiang Wang, yiqiang.wang@ukaea.uk
Tay Sparks, txs971@student.bham.ac.uk

Outline

- Requirements of nuclear fusion materials
- Eurofer 97 as a structural material
- In-Situ XRD Tensile Testing of E97/ODS E97
- Conclusions

Introduction

- Extreme harsh environments: 10-200 dpa neutron irradiation, 300-800 °C
- ODS low activation F/M steel (e.g. ODS Eurofer 97) is a promising candidate structural support to the breeder blanket .

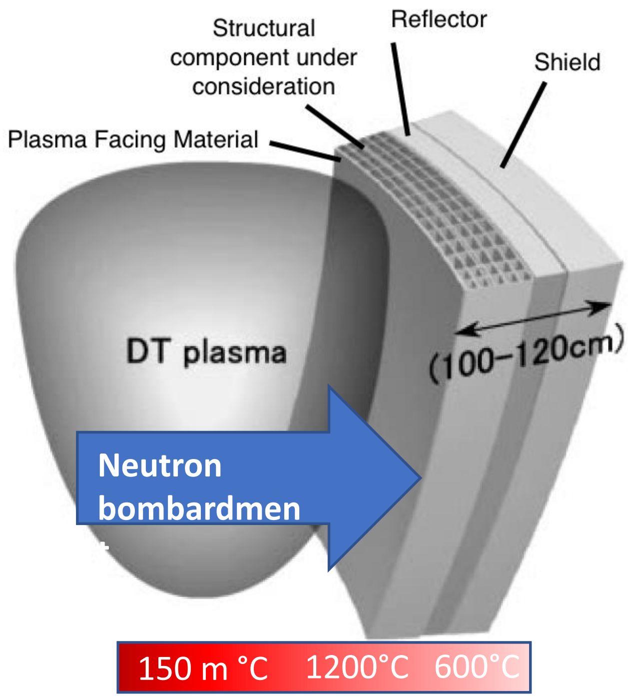

T. Muroga Mat. Transact. 46 3 (2005) pp405-411

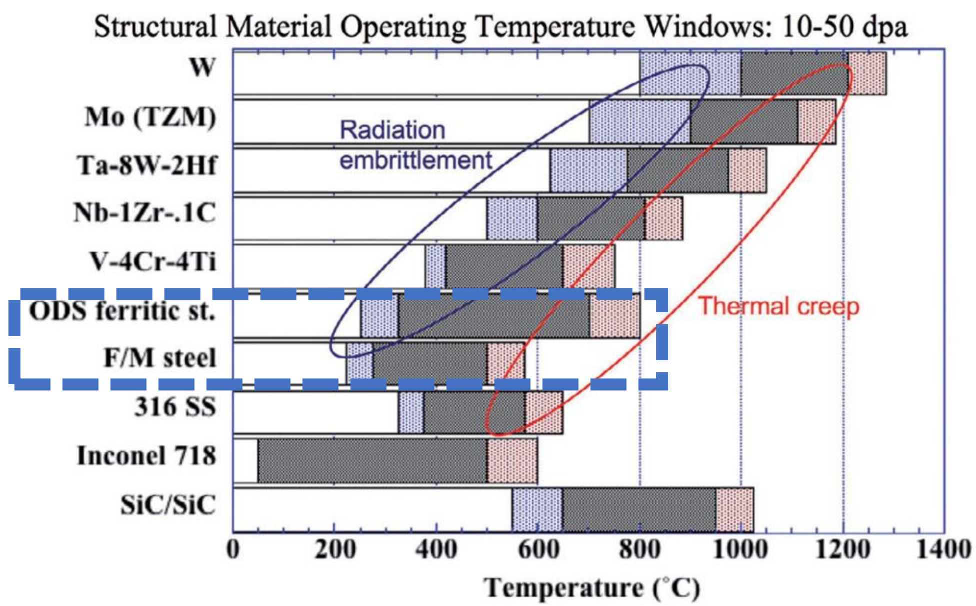

S.J. Zinkle et al, Materials Today 12, 11 (2009) pp12-19

ODS Eurofer97 Steel

- E97: FM steels alloyed with low activation elements
- ODS E97: ODS particles (Y_2O_3) improve thermal creep of Eurofer97 steel

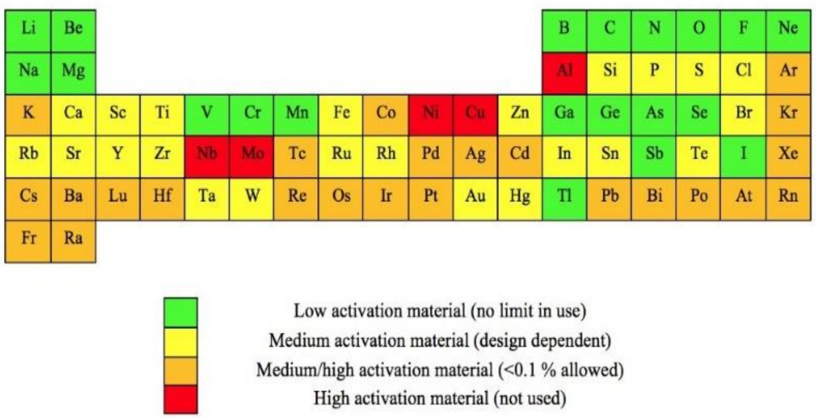

Alloying element	Eurofer	ODS Eurofer
Cr	8.95	8.92
W	1.06	1.11
Mn	0.55	0.41
V	0.202	0.193
Ta	0.12	0.08
C	0.11	0.07
Si	0.03	0.11
Mo	0.005	0.037
Y_2O_3	-	0.3

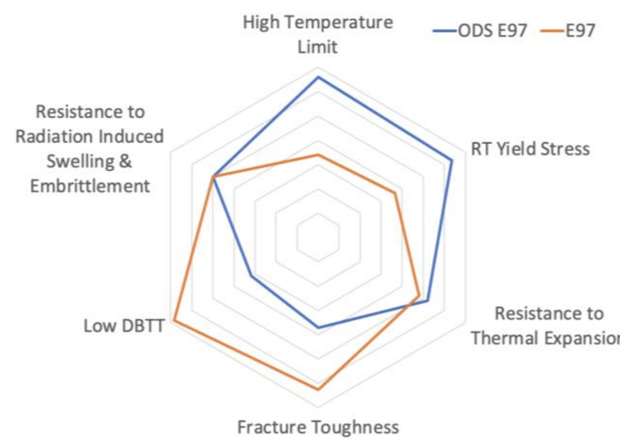

Comparation of E97 and ODS E97

In-Situ XRD Tensile Testing at Diamond Light Source

- High temperature tensile testing was performed on Eurofer and ODS Eurofer 97 steels
- High energy X-ray diffraction was used to monitor the microstructure evolution

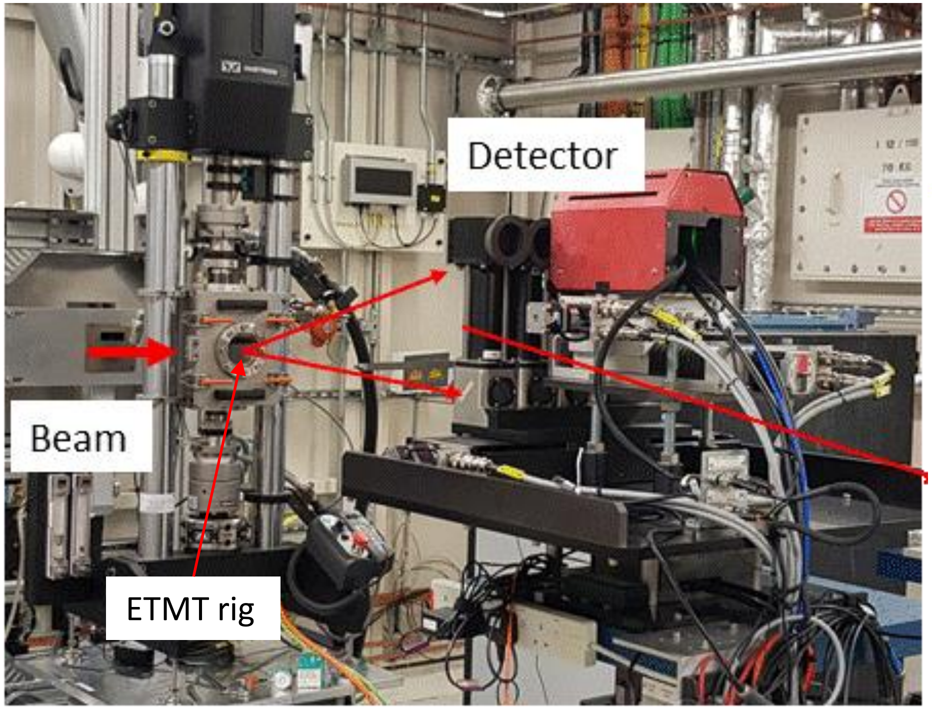

ETMT at I12 Diamond Light Source

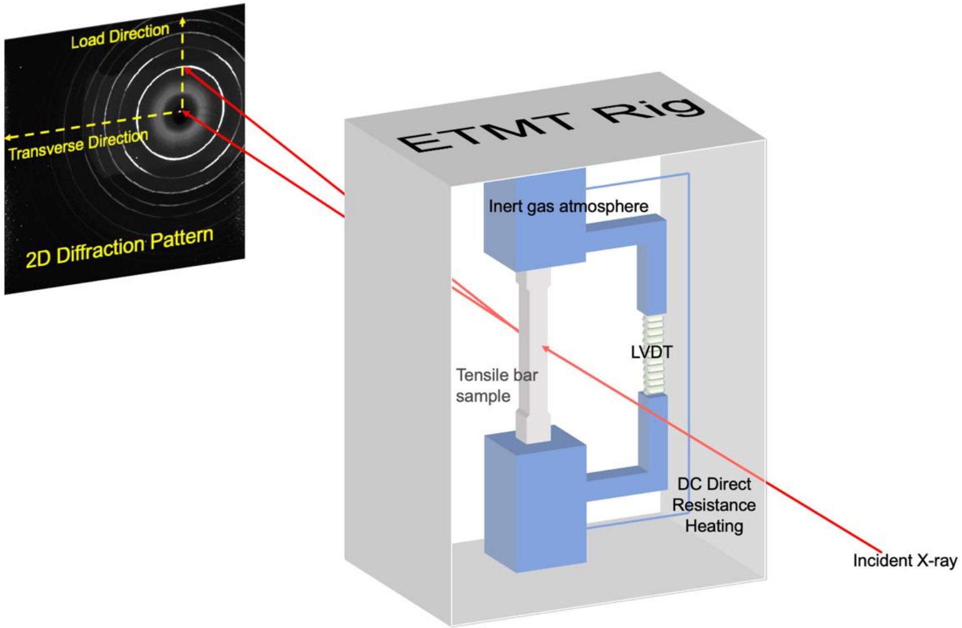

High temperature mechanical properties

- ODS particles strengthen Eurofer97 but degrade total elongation
- Strengthening effect lessens with increased temperature

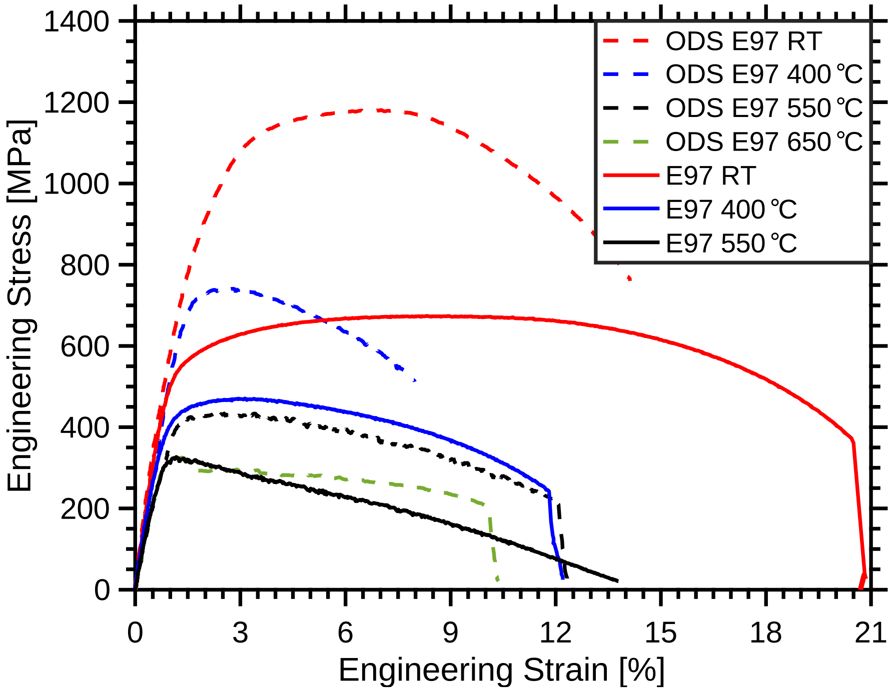

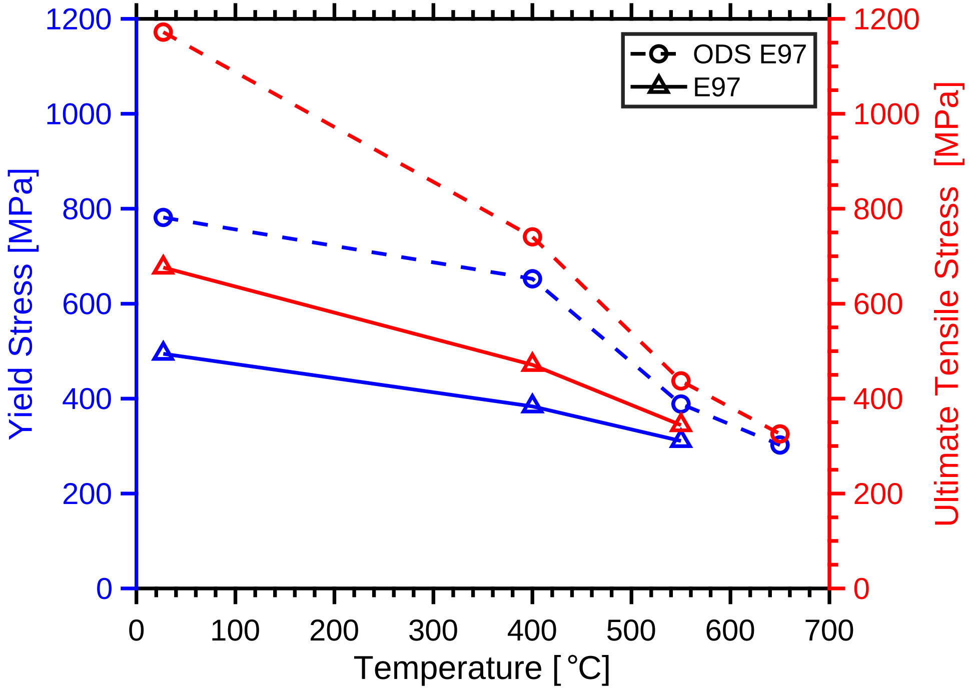

Lattice Strain Evaluation

Lattice strain: $\varepsilon_{hkl} = \frac{d_{hkl} - d_{hkl,0}}{d_{hkl,0}}$

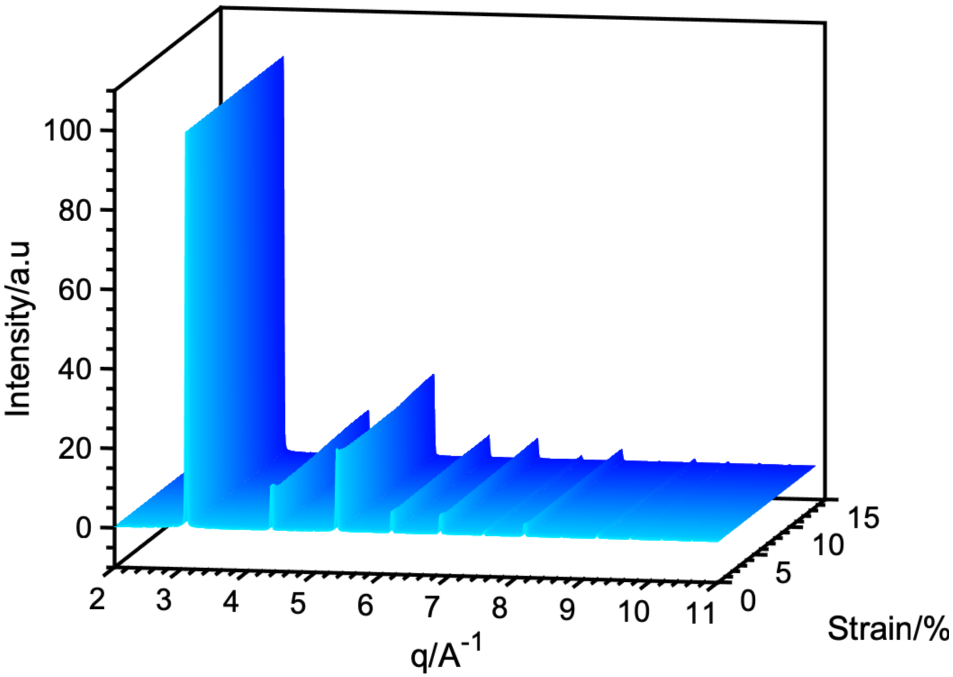

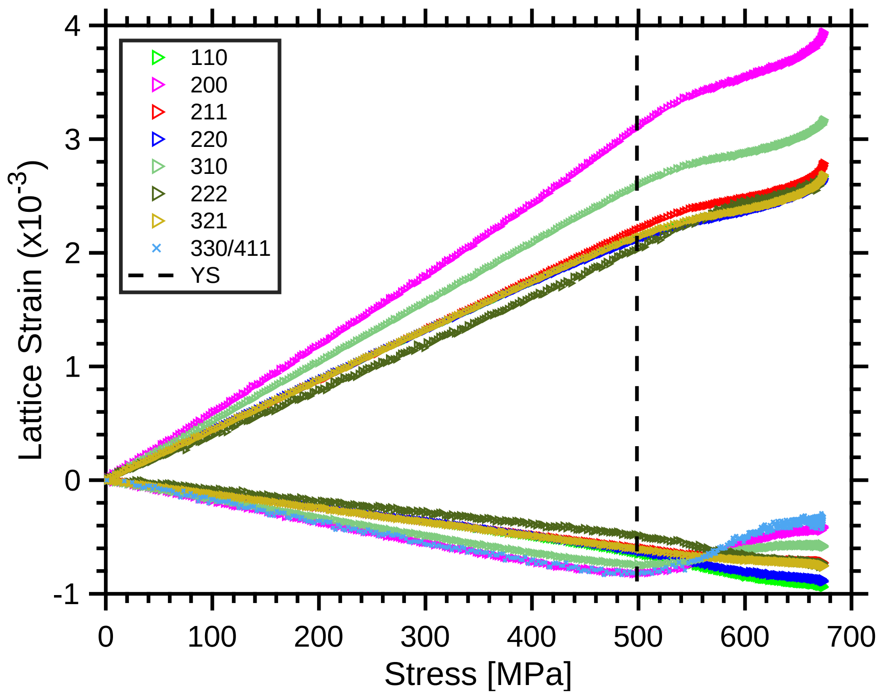

Single crystal elastic constants (SCEC)

- SCECs are critical for modelling material tensile response

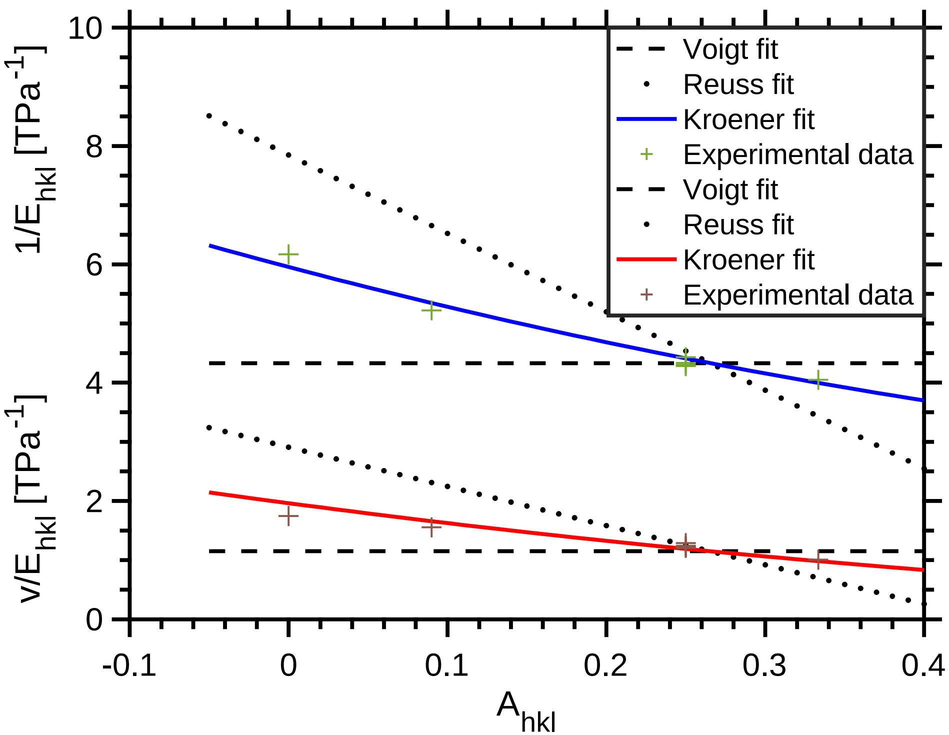

Elastic tensor of BCC:

$$\begin{bmatrix} C_{11} & C_{12} & C_{12} & 0 & 0 & 0 \\ C_{12} & C_{11} & C_{12} & 0 & 0 & 0 \\ C_{12} & C_{12} & C_{11} & 0 & 0 & 0 \\ 0 & 0 & 0 & C_{44} & 0 & 0 \\ 0 & 0 & 0 & 0 & C_{44} & 0 \\ 0 & 0 & 0 & 0 & 0 & C_{44} \end{bmatrix}$$

Sample	C11 [GPa]	C12 [GPa]	C44 [GPa]
E97 RT	226±4	133±4	121.1±0.3
E97 400C	193±7	129±7	105.9±0.5
E97 550C	180±10	124±8	105.3±0.7
ODS E97 RT	239±2	136±2	113.2±0.2
ODS E97 400C	179±5	110±5	84.9±0.4
ODS E97 550C	130±10	100±10	114±1
ODS E97 650C	104±8	75±8	122±2

Polycrystalline moduli

- Mechanical anisotropy is accentuated at elevated temperature

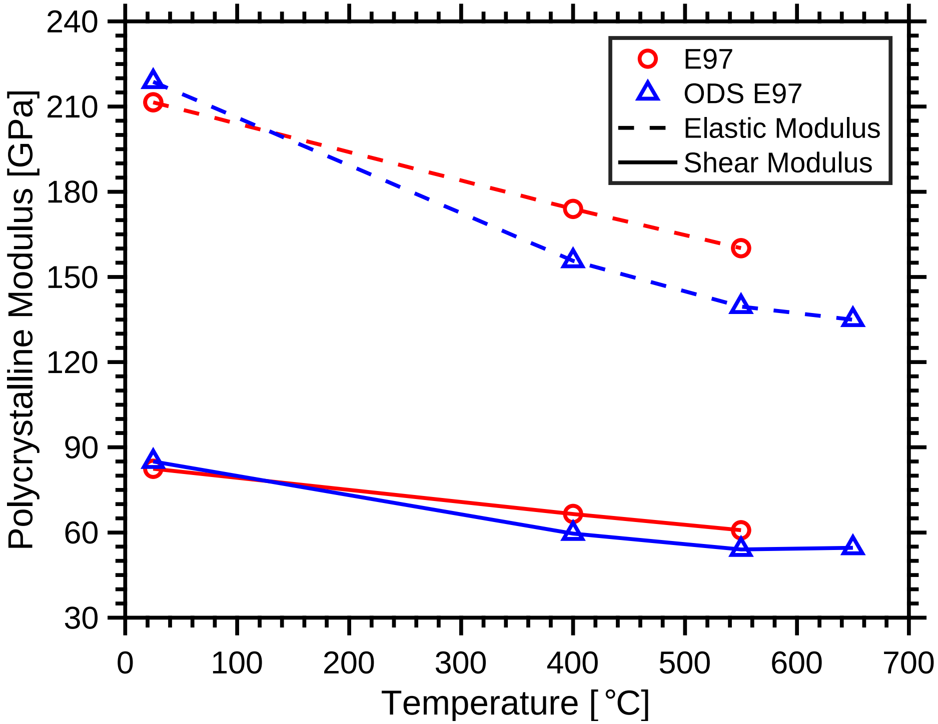

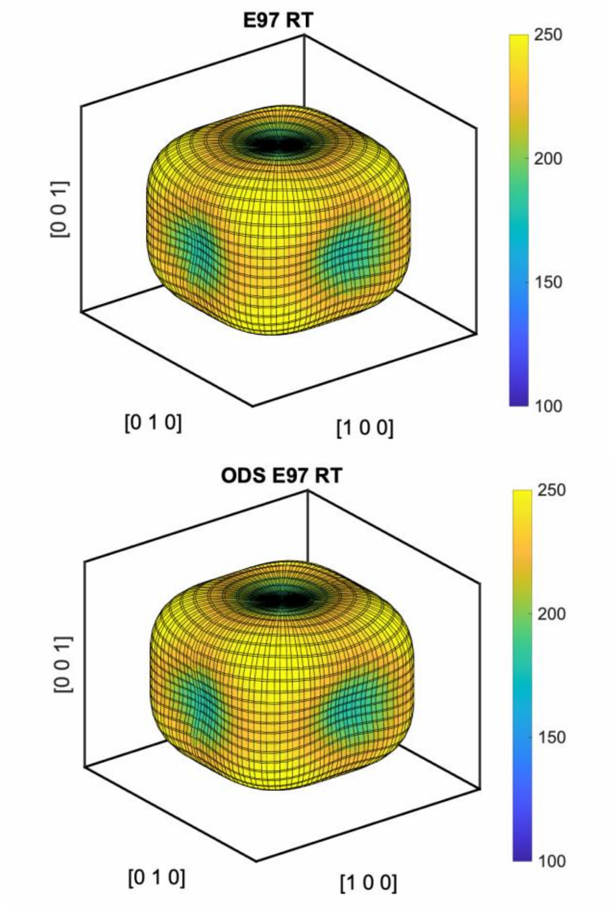

Dislocation density

- Instrumental broadening, crystallite size broadening, dislocation broadening

$$\Delta K \approx {}^{0.9}/_{D} + \sqrt{{}^{\pi M^2 b^2}/_{2}} \cdot \rho^{0.5} \cdot KC^{0.5} + OK^2C$$

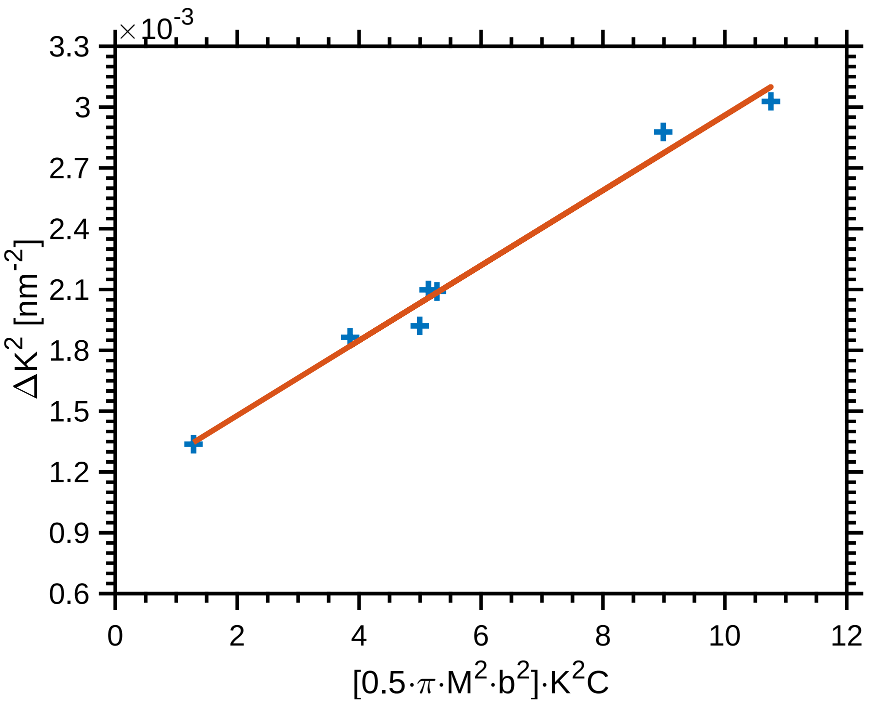

Dislocation density evolution (4 stages)

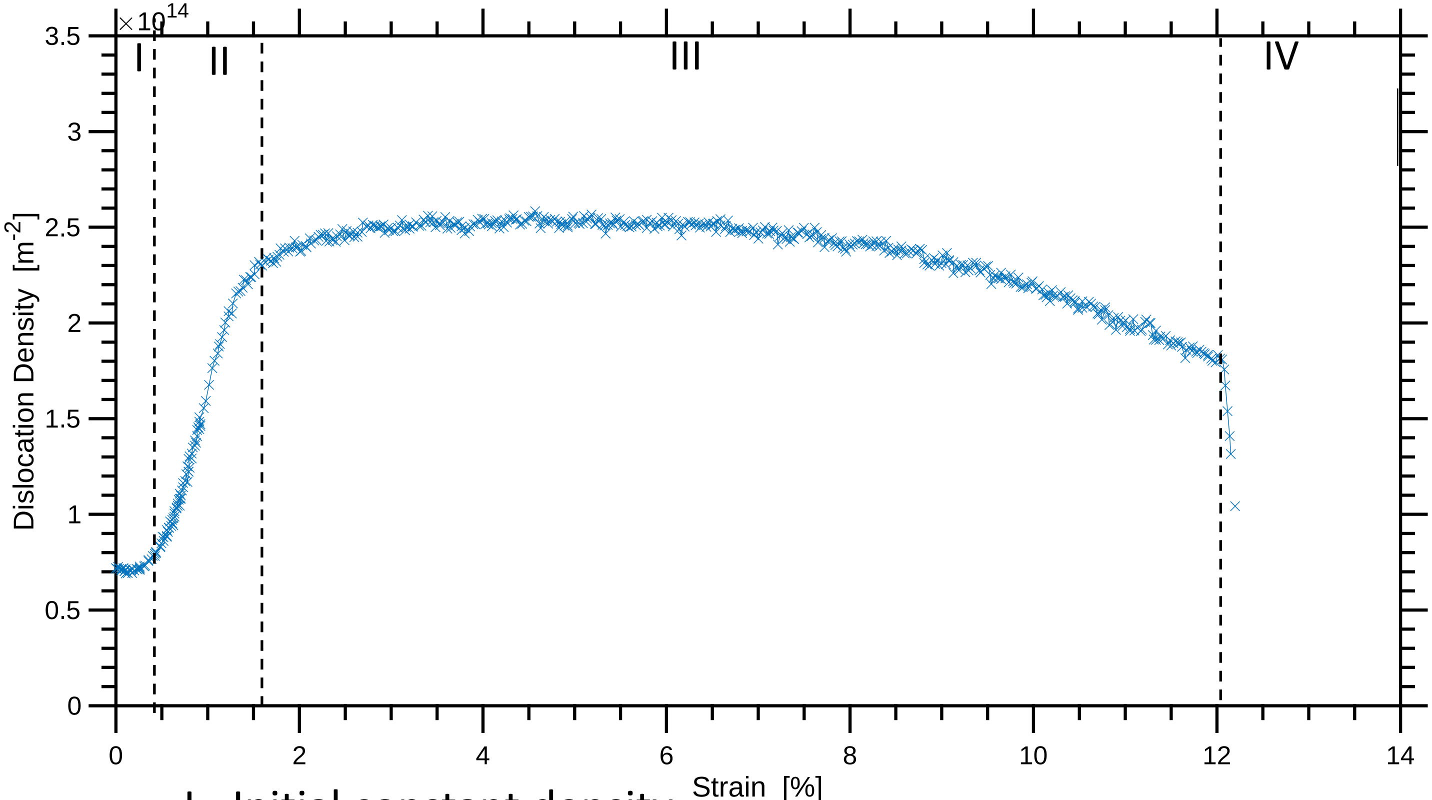

I - Initial constant density

II - Onset of rapid density multiplication

III - Constant or slow growing dislocation population

IV - Final dislocation fall with unloading at fracture

Dislocation density evolution

- Increased temperature increases dislocation annihilation, decreases dislocation density
- ODS particles act as nucleation points for dislocations, and pin dislocation movement
  - Increased initial density
  - Increased rapid multiplication

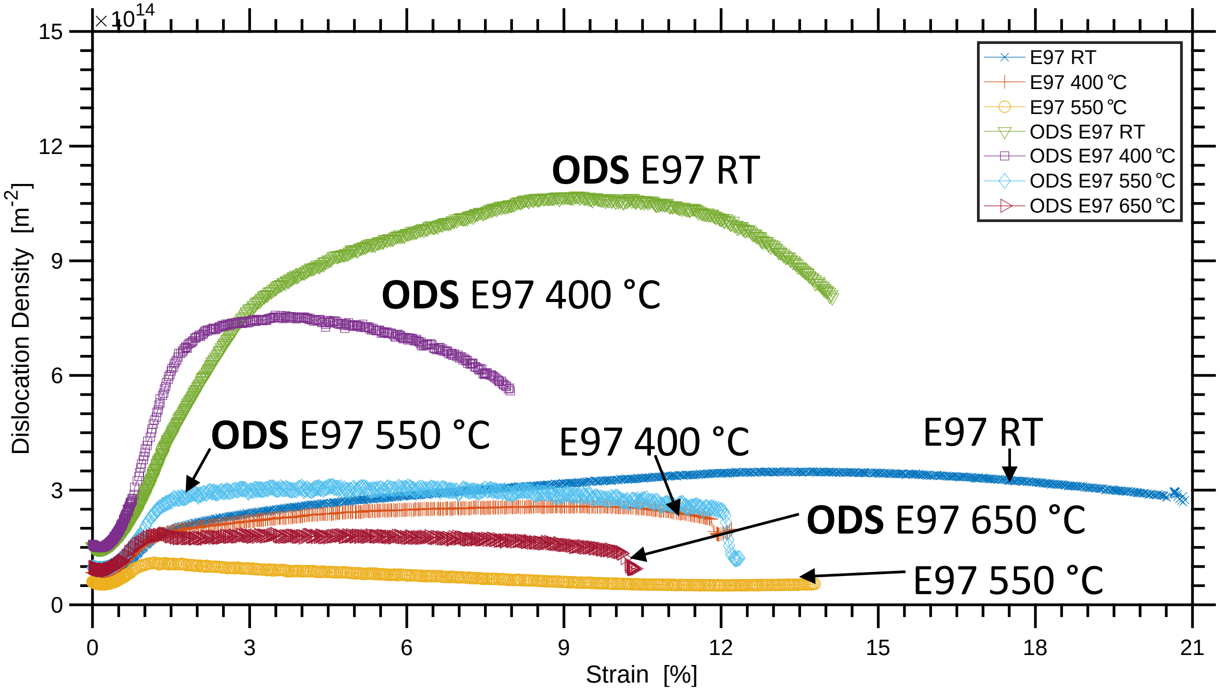

Constitutive Flow Analysis

- Dislocation based flow modelling was used to predict yield strength at different temperatures

Temperature driven

$$\sigma_y = \sigma_{SS} + \sigma_{HP} + \sigma_{BH} + \sigma_K + \sigma_{ARW} + \sigma_{CC}$$

Particle strengthening

$$\sigma_{SS} = 0.00689 \sum kC^n$$

Solid Solution Strengthening

$$\sigma_{BH} = M\theta G(T) b \rho^{0.5}$$

Dislocation strengthening

$$\sigma_{CC} = \frac{k_b T D^3 \dot{\varepsilon}}{47\Omega \delta_B D_B} \exp\left({}^{Q_B}/_{RT} \right)$$

Creep driven by diffusion along grain boundaries

$$\sigma_{HP} = \sigma_0 + \sigma_D = \sigma_0 + \left(\frac{G(T)}{G(RT)} \right)^{0.5} \cdot \frac{K}{\sqrt{D}}$$

Effect of grain size and fundamental lattice friction

$$\sigma_{ARW} = 0.9M \frac{G(T) b {R_T}^{1.5}}{L\left(2\sqrt{2} + {R_T}^{1.5}\right)}$$

Dislocation particle interaction – Climb around

$$\sigma_K = 0.9M \frac{\left[\ln\left({}^{\pi d}/_{b} \right)\right]^{1.5} G(T) b}{\left[\ln\left({}^{L}/_{b} \right)\right]^{0.5} \cdot \left[L - \left({}^{\pi d}/_{4} \right)\right] \cdot [4\pi(1 - \upsilon)]}$$

Dislocation-Particle Interaction – Orowan Bowing

Constitutive Flow Analysis

- Good agreement between experimental measurements and modelling
- Large fall in YS beyond 400°C correlated to change of obstacle depinning – bowing to climb

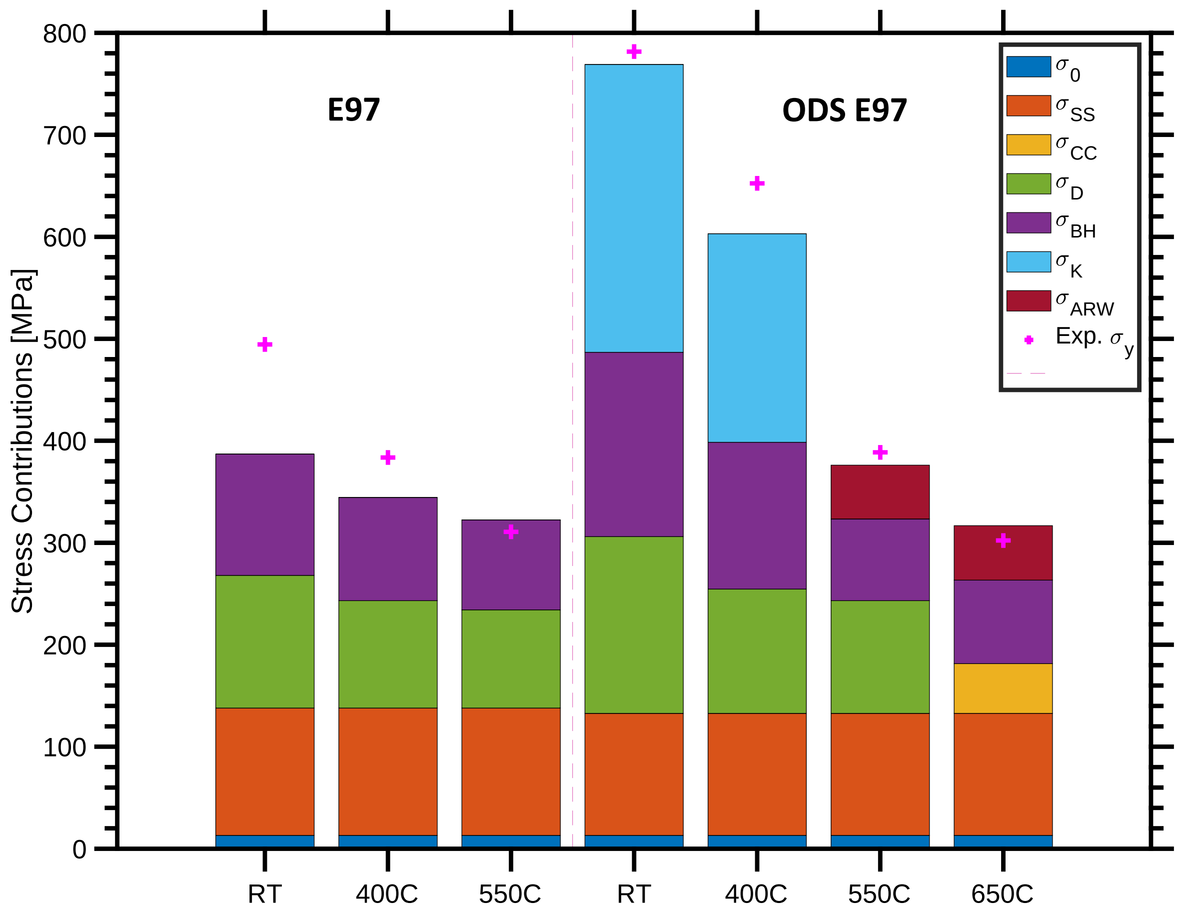

Conclusions

- Single crystal elastic constants experimentally generated for Eurofer97 and ODS Eurofer97
- Polycrystalline elastic properties evaluated
- ODS particles noted as effective dislocation pins and generators
- Degradation of yield stress in ODS E97 correlated to:
  - a fall in the pinning efficiency of ODS particles above 400°C
  - the breakdown of Hall-Petch strengthening above 550°C

Acknowledgements

- Funding for this work was provided by the United Kingdom Atomic Energy Authority (UKAEA) and the University of Birmingham School of Metallurgy & Materials.
- Dr. Wang and Dr. Gorley would also like to acknowledge the RCUK Energy Programme [grant EP/T012250/1] and the UK Government Department for Business, Energy and Industrial Strategy for time and resources.
- We acknowledge Diamond Light Source for time on the I12 beamline under proposal [EE19251].